Study of solvent debinding parameters for metal injection moulded 316L stainless steel

IOP Conf. Series: Materials Science and Engineering **257** (2017) 012035 doi:10.1088/1757-899X/257/1/012035

Study of solvent debinding parameters for metal injection moulded 316L stainless steel

M F F A Hamidi[1*], W S W Harun[2], N Z Khalil[2], S A C Ghani[2], M Z Azir[3]

[1] Institute of Postgraduate Studies, Universiti Malaysia Pahang, Lebuhraya Tun Razak, 26300 Gambang, Kuantan, Pahang, Malaysia
[2] Green Research for Advanced Materials (GramsLab), Human Engineering Group, Faculty of Mechanical Engineering, Universiti Malaysia Pahang, 26600 Pekan, Pahang, Malaysia
[3] DRB-HICOM University of Automotive Malaysia, Kawasan Perindustrian Peramu Jaya, 26600 Pekan, Pahang, Malaysia

*Corresponding author: faizulfarhan06@gmail.com

Abstract. Solvent debinding is one of a crucial stage in Metal Injection Moulding (MIM) process. This process begins with the removal of the soluble binder components by using solvents such as heptane or hexane. In solvent debinding process, unsuccessful to achieve maximum binder removal will cause a defect to the compact such as crack and swelling. So to have an optimum solvent debinding parameters are very important to improve the quality of the compact. Optimisation of solvent debinding process parameters for MIM of Stainless Steel 316L has been testified in this study. Gas atomised stainless steel 316L powder was mixed with a multicomponent binder in a twin blade mixer at a temperature of 150 °C for 90 minutes. The feedstock was successfully injected at the temperature of 150 °C. The green compacts were kept in n-heptane for eight different debinding times ranging between 30 to 240 minutes at temperatures of 40, 50, 60 and 70 °C to remove the primary binder components. From the result, the optimum temperature and time for solvent debinding were recorded at 60 °C and 240 minutes. Solvent debinding temperature and time give a significant effect on the rate of paraffin wax removal.

1. Introduction

The fabrication of biocompatible metals as implant devices is restricted because of the rather high costs of raw materials, complex design geometry, and limitations of the current fabrication process. Metal injection moulding (MIM) could serve as an alternative means to overcome these problems. One of the reasons is that MIM process could reduce production costs due to its net-shape fabrication advantages, befitting for manufacturing of small parts, and combine high part complexity with large production quantities [1-4]. This technique was procured and adapted from the plastic injection moulding process, of which small metal particles replaced a significant volume fraction of plastic [5-8].

In MIM technology, there are four processing stages which are, mixing of powders and binders to produce feedstock, injection moulding, debinding, and sintering.The third step was the debinding process where all the binders will be extracted from the compacts. This process is crucial as it can influence MIM processes and the ultimate quality of the products. Long debinding times combined with relatively high tendency of compact distortion are the main challenge for MIM process [9-12]. To increase the rate of binder removal while preventing the compacts from defects, debinding is typically conducted in multiple stages, namely solvent and thermal debinding. For solvent debinding process, it

has been studied first to perforate the binder structure before proceeded to thermal debinding stage [13-15]. The solvent debinding process was popularised to the metal injection moulding industries during the 1980s. In this process, it began with the removal of the soluble binder components by using solvents such as heptane or hexane [16, 17].

In this study, an experiment was conducted to optimise the solvent debinding parameters of 316L stainless steel. 62 vol.% powder loading of 316L stainless steel were mixed with the multi-component binders by using twin blade mixer. The green compacts were kept in vaporised n-heptane solvent at various time and temperatures. The microstructure of green and debound compacts were observed using SEM. It is expected that higher solvent debinding temperature and time will increase the removal rate of the primary binders, particularly paraffin wax.

2. Experimental Method

2.1 Material

The gas atomized 316L Stainless Steel (SS) alloy powder provided by Osprey Co, the UK with the mean particle size of 11.4 μm was utilised in this study. Chemical composition and particle morphology of the powder are shown in Table 1 and figure 1 respectively.

Table 1. Chemical composition of gas atomized 316L SS.

Element	Wt.%
Cr	16.7
Ni	10.3
Mo	2.2
Mn	0.99
Si	0.69
P	0.02
C	0.01
S	0.05

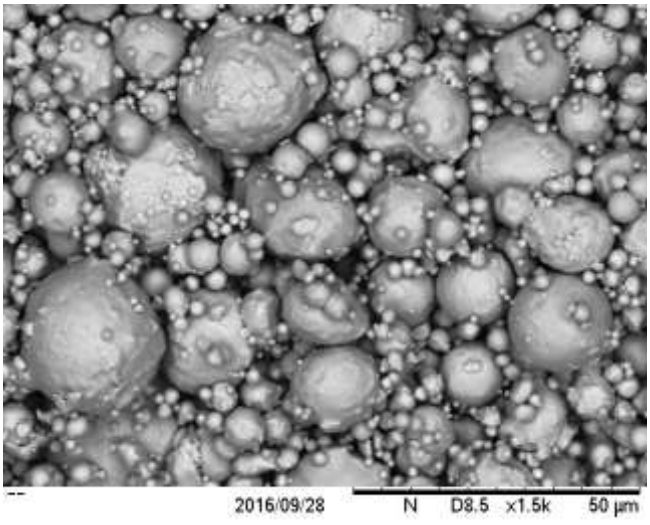

Figure 1. Particle morphology of 316L SS powder.

2.2 Feedstock Preparation

A formulation 62 vol % powder loading of stainless steel powders was prepared. 62 vol % powder loading was obtained from the preliminary investigations performed to estimate the optimum powder loading. A multicomponent binder system used to formulate the feedstock consists of Paraffin Wax (PW), Polypropylene (PP), and Stearic Acid (SA). Table 2 shows the composition of the

multicomponent binder used in this work. Twin blade type mixer at a rotational speed of 70 rpm at 150 °C for 90 min has been utilised to mix the feedstock.

Table 2. Binder system for SS 316L.

Binder Components	Composition (%)
Paraffin wax (PW)	70
Polypropylene (PP)	25
Stearic acid (SA)	5

2.3 Thermal analysis of the feedstock

To identify the melting temperature for each binder component, Differential Scanning Calorimetry (DSC) has been used. The suitable temperature for mixing, injection moulding and solvent debinding also can be determined from this analysis. DSC analysis has been performed on an NETZSCH DSC 214 Polyma DSC21400A-01717-L equipment. The heating rate was set at 10°C/min and conducted under nitrogen atmosphere.

2.4 Injection Moulding of Feedstock

Injection process for feedstock was performed on a Nissei NS20-2A injection moulding machine to fabricate tensile shape compacts. The green compacts were produced by injection moulding at 150 °C. There is no defects were observed on the green compact after it have been checked physically.

2.5 Solvent Debinding

For solvent debinding process, wicking debinding technique was applied by using fine Al_2O_3 powders [13]. At this stage, the primary binder which is paraffin wax will be extracted from the green compacts. Compacts were kept in a solvent bath of the vaporised heptane at 40, 50, 60 and 70 °C for 30 to 240 minutes. The schematic diagram for solvent debinding process is shown in figure 2.

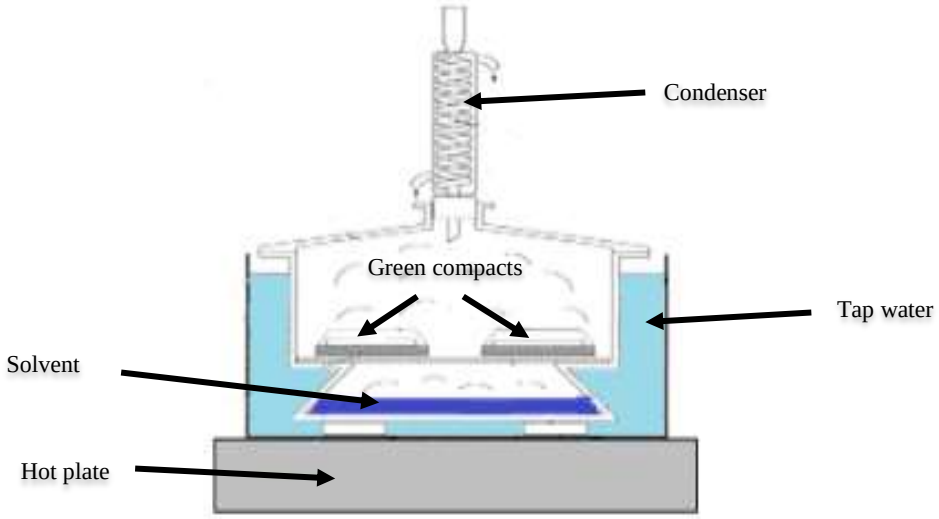

Figure 2. Schematic diagram for solvent debinding process.

2.6 SEM Analysis

The micrograph for green and solvent debound compacts was analysed using Scanning Electron Microscopy (SEM). This analysis also used to verify the complete leaching and homogenous distribution of primary binder from the solvent debound compacts correspondingly.

3. Results and Discussion

The green compacts were well moulded via Nissei NS20-2A injection moulding machine. Figure 3 shows a defect-free green compacts. The mould and injection temperatures were 40°C and 150°C respectively.

Figure 3. Defect-free 316L SS green compacts.

3.1 Solvent Debinding

To extract the soluble binders, solvent debinding was carried out by keeping the green compacts in the solvent bath of vaporised n-heptane solution at different temperatures and times. This technique has been chosed because paraffin wax can be dissolved in vaporised n-heptane. During solvent debinding process, open pore channels will be produced on the debound compacts, which allow the diffusion process of the remaining binder in the second debinding process. The schematic diagram for the solvent debinding process is shown in figure 4. This schematic diagram suggests how the binders was extracted from the green compacts due to the capillary forces that happened when these compacts start to dissolved by the vaporised solvent [18].

The indicator to determine the suitable temperature during solvent debinding which is the melting point of the binders was verified by using DSC analysis. Figure 5 depicts the DSC analysis result for the feedstock .From Figure 5, there was three peak melting temperature of the multicomponent binders have been observed which are 58 and 168 °C. Each peak shows an endothermic reaction. It is envisaged that peaks at lower temperature (58°C) correspond to the the melting point of Paraffin Wax and Stearic Acid whereas the peak at a higher temperature correspond to the melting point of Polypropylene. The solvent debinding temperature directly affected the diffusivity and solubility of the binders in the solvent. Thus, the selection of solvent debinding temperature should be guided by the melting temperatures of the binders. The melting temperature of Paraffin wax and Stearic acid were used as a reference at this stage.

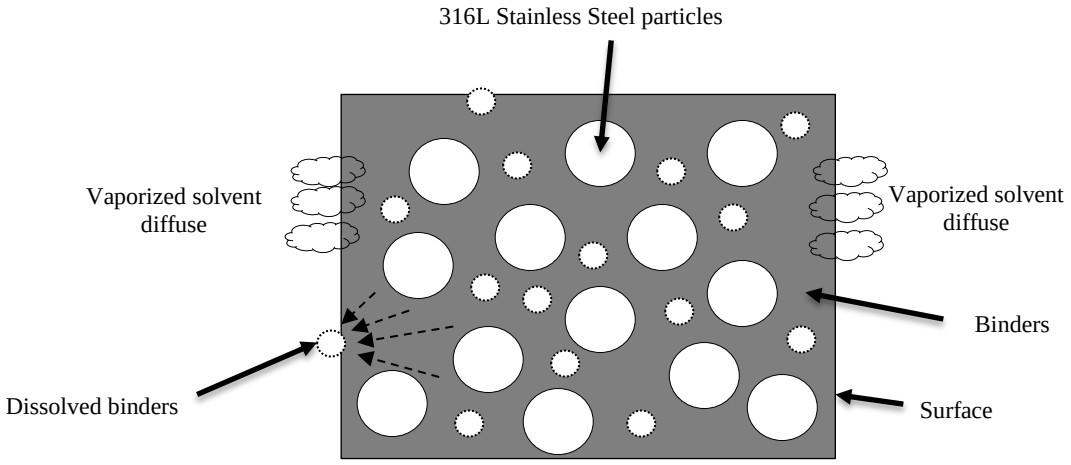

Figure 4. The schematic of solvent debinding stage.

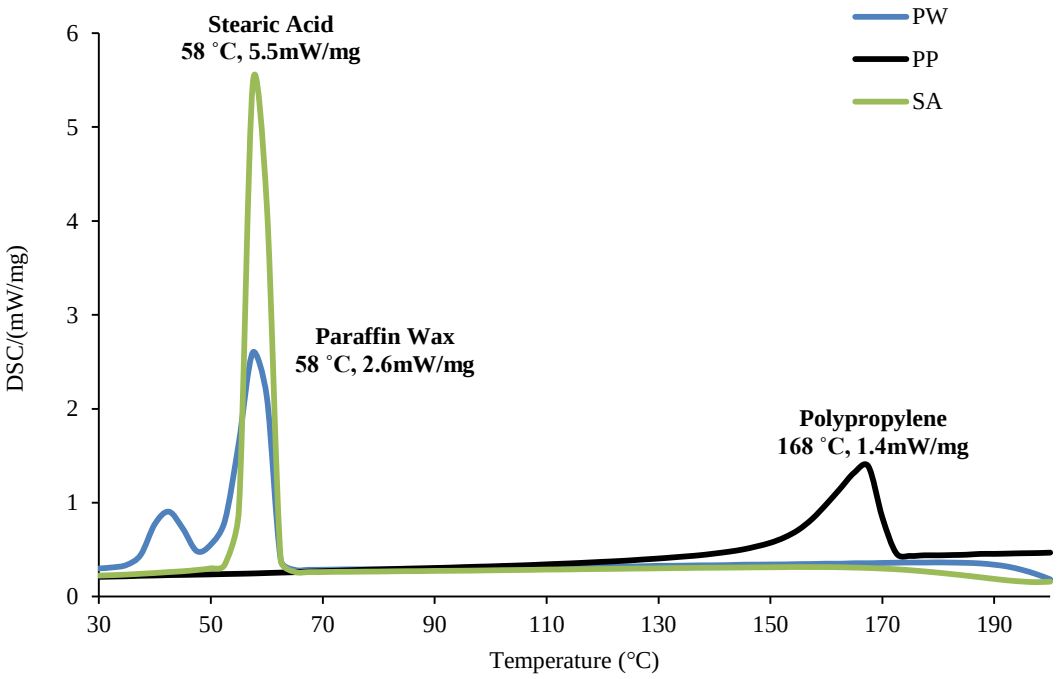

Figure 5. Differential Scanning Calorimetry analysis.

In this work, wicking debinding technique was applied by using Al_2O_3 powder. From the observation, at the end of the solvent debinding process, removed paraffin wax changed the Al_2O_3 powder from white to yellowish colour as shown in figure 6. It was suggested by [19] that this observation is due to the capillary suction that causes the soluble binder move toward the wicking powder as it is in contact with the powder.

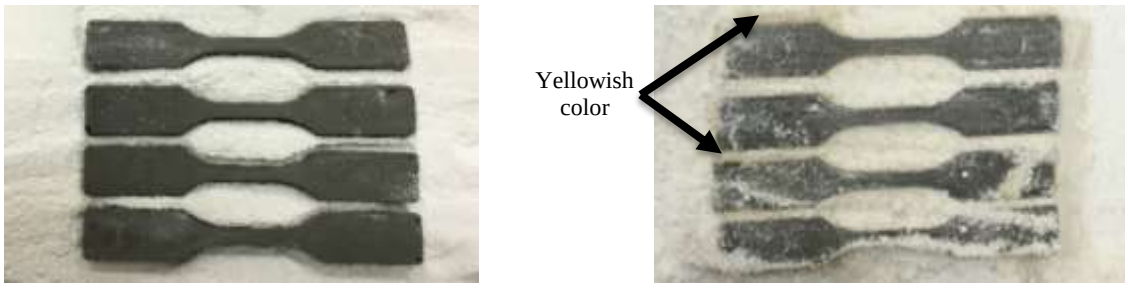

(a) (b)

Figure 6. Solvent debinding a) before solvent debind, b) After solvent debind.

To identify the optimum solvent extracted condition, four (4) debinding temperatures were chosen which were 40, 50, 60 and 70°C. The debinding time was varied between 30 to 240 minutes to observe the optimum extraction time. Figure 7 presents the influence of solvent debinding temperature and time on the rate of Paraffin Wax removal. Mass loss of the binder (M_{loss}), which is the paraffin wax, was calculated based on the following equation:

$$M_{loss} = \frac{Mi - Mf}{Mi} \text{ x } 100 \quad (1)$$

Where *Mi* is the mass of green compact and *Mf* is the mass of debound compact. It can be determined that the percent of paraffin wax loss from the green compacts is increased with the increases in

debinding temperature, particularly in the first 30 minutes of the process. At this period, the rate of binder loss is extremely fast as the vaporised heptane were directly in contact with the binder on the surface of the compacts. Then, before the vaporised n-heptane dissolved the binder, it firstly diffused deeply into the green compacts. Thus, the rate of binders' loss significantly slowed till it achieved a plateau region after 210 to 240 minutes. This phenomenon occurred when a dynamic equilibrium has been reached between the solvent and binders as the percentage of paraffin wax removal maintained unchanged. This phenomenon also has been explained by the previous researcher [20].

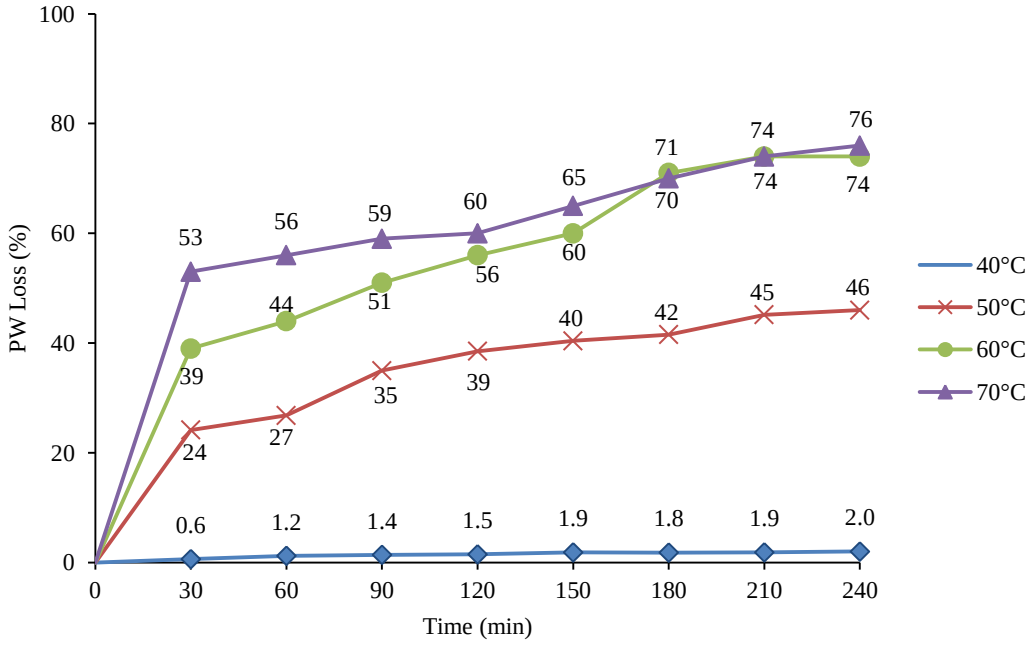

Figure 7. Effect of solvent debinding temperature and time on the rate of paraffin wax removal.

3.2 Defects

From Figure 7, 74 % and 76 % wax was removed at temperature 60 °C and 70 °C after 240 minutes. Both temperatures can be considered as the optimum temperature for solvent debinding process as they recorded the highest percent of paraffin wax loss from the green compacts. The amount of Paraffin Wax loss for both temperature also was acceptable because too much binder loss will cause the compact to become fragile and difficult to handle. However, for the first 30 minutes, 53 % of Paraffin Wax has been removed at temperature 70 °C, and it is higher compared to temperature 60 °C which recorded 39 % of Paraffin Was loss. The maximum amount of binder loss for 70 °C at the early stage of the debinding process inappropriate for the green compacts as some of the compacts were found to be broken as shown in figure 8.

Figure 8. Damaged compacts.

Too high extracting temperature was not appropriate for solvent debinding process as it will affect the quality and can cause defects on the debound compacts. This result also align with previous work by [21] and [18] where they found that, after the debinding temperature had been increased higher than 60 °C, swelling and crack were generated on the surface of the compacts. They also explained that more binders are diffused and melted speedily out from the compacts when the debinding temperature was higher than the melting temperature of a binder hence leading to the initiation of defects on the debound compacts. The defects that experienced by the compacts also might be because of the thermal expansion of the binders because of the reaction at higher temperature among the binders and solvent. In this work, most of the compacts were cracked at 70 °C. Therefore, 60°C has been set as the optimum solvent debinding temperature where high percent rate of paraffin wax removal was recorded. After 240 minutes, 74 % of paraffin wax loss was achieved, which demonstrated in the creation of defect-free compacts.

3.3 SEM Analysis

SEM micrograph in figure 9 shows a cross-sectional view of the green and debound compact. The SEM micrograph for the debound compact was taken from the green compact that was debound in the optimum condition which is at 60°C for 240 minutes. It is observed that binders were uniformly distributed within the 316L stainless steel powders to prevent it from oxidation and maintain the shape of the compacts as shown in Figure 9(a). Uniform binders' distribution also can be observed in the green compact. Figure 9(b) presents the open pores channels that were produced after the removal of paraffin wax. Some were inter-particle pores, and several were in the interior of the binder, indicating that paraffin wax, polypropylene and stearic acid were interacted and mixed to a degree and that a few soluble binders were removed. This result has proved the effectiveness and success of n-heptane as a solvent in extracting the paraffin wax from the green compacts. After 240 minutes of solvent debinding process, a significant amount of paraffin wax has been extracted, leaving the remaining polypropylene either in the contact areas or as whiskers holding particles together. From the SEM observation, the open pore channels also have been developed at the centre of the compact. This shows that the penetration of vaporised was reached at the core of the compact. With these open pore channels, the remaining binders especially polypropylene can be removed easily without affecting the compacts in the thermal debinding stage. If there are no open pores were produced in this stage, the backbone binders especially polymer cannot be removed easily in the thermal debinding stage. The binders will keep pushing the compact surface outward and cause the surface of the compacts become rough and also have a potential to produce a crack on the compact [22]. Therefore, this process can help in shortening the thermal debinding process and maintained the integrity of the compact [17].

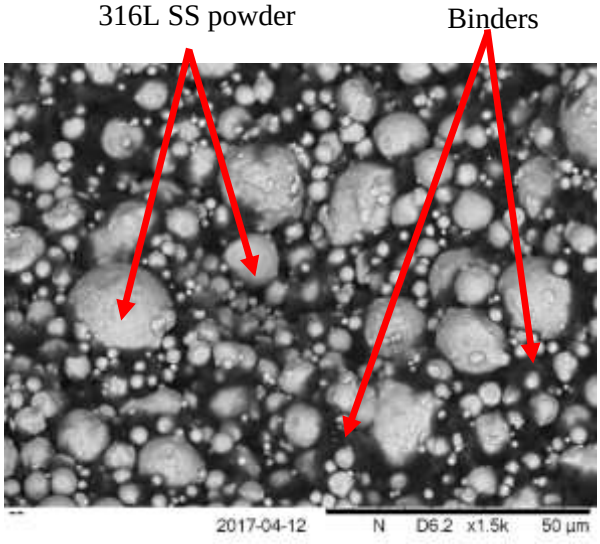

(a)

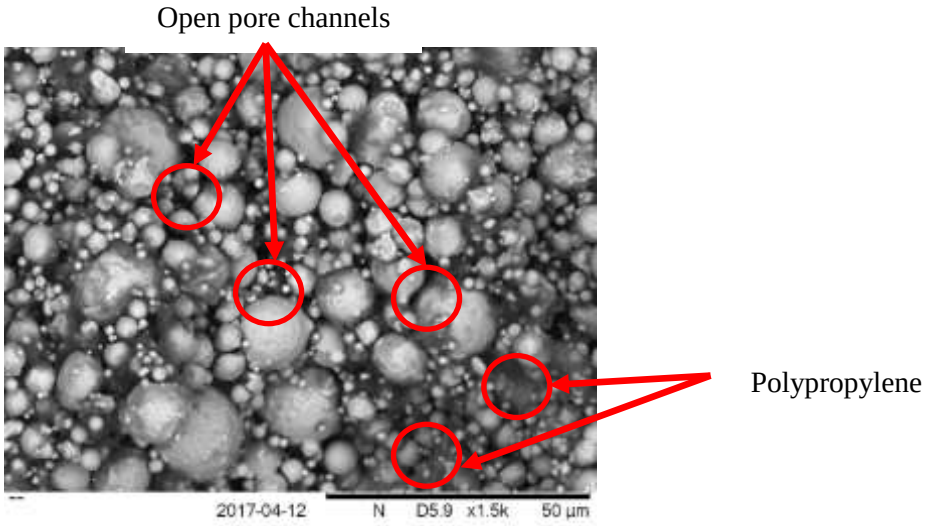

(b)

Figure 9. SEM micrograph (a) green compact (b) solvent debound compact.

4. Conclusions

This work concludes the following:

1) To attain the optimum parameters for solvent debinding process, the green compacts were solvent debound at different temperature and times. From the experiment, temperature and time proved to have a significant effect on the mass loss of paraffin wax as the removal rate increased with the increase of temperature and times particularly in the first 30 minutes.
2) The optimum solvent debinding parameters have been verified. Solvent debinding at 60°C for 240 minutes were considered as the optimum parameters for solvent debinding process because of the adequate quantity of paraffin wax loss. The total percentage of paraffin wax removal for this condition was recorded at 74 %.
3) Solvent debinding temperature at 70°C showed a rapid removal of paraffin wax and generated a defect which is crack on the compact. This might be due to thermal expansion of the binders as a result of the reaction at higher temperature among the binders and solvent.
4) From SEM analysis for green compact, the binders were very well mixed with the 316L stainless steel powder. For a debound compact, a lot of open pore channels were produced where they can help on removing the remaining binders in the thermal debinding stage easily.

Acknowledgments

Universiti Malaysia Pahang fully supports the resources and facilities for this work. The author W.S. W. Harun would like to acknowledge the funding of the internal grant of Universiti Malaysia Pahang RDU141101, RDU140354, RDU150337, PGRS160383, PGRS170388 and the support of Research Acculturation Collaborative Effort (RACE) RDU151314 and Research Acculturation Grant Scheme (RAGS) RDU151404 provided by the Ministry of Higher Education, Malaysia. Besides that, the project also has been supported by Qatar National Research Fund NPRP88762375 (UIC161504).

References

[[1] Santos P F, Niinomi M, Liu H, Cho K, Nakai M, Itoh Y, Narushima T and Ikeda M 2016 Fabrication of low-cost beta-type Ti–Mn alloys for biomedical applications by metal injection molding process and their mechanical properties *Journal of the Mechanical Behavior of Biomedical Materials* **59** 497-507

[2] Hayat M D, Goswami A, Matthews S, Li T, Yuan X and Cao P 2017 Modification of PEG/PMMA binder by PVP for titanium metal injection moulding *Powder Technology* **315** 243-9

[3] Hausnerova B, Mukund B N and Sanetrnik D 2017 Rheological properties of gas and water atomized 17-4PH stainless steel MIM feedstocks: Effect of powder shape and size *Powder Technology* **312** 152-8
[4] Marçal R L S B 2016 *Reference Module in Materials Science and Materials Engineering*: Elsevier)
[5] Aggarwal G, Smid I, Park S J and German R M 2007 Development of niobium powder injection molding. Part II: Debinding and sintering *International Journal of Refractory Metals and Hard Materials* **25** 226-36
[6] Raza M R, Ahmad F, Muhamad N, Sulong A B, Omar M A, Akhtar M N and Aslam M 2016 Effects of solid loading and cooling rate on the mechanical properties and corrosion behavior of powder injection molded 316 L stainless steel *Powder Technology* **289** 135-42
[7] Zhao D, Chang K, Ebel T, Nie H, Willumeit R and Pyczak F 2015 Sintering behavior and mechanical properties of a metal injection molded Ti–Nb binary alloy as biomaterial *Journal of Alloys and Compounds* **640** 393-400
[8] Mariot P, Leeflang M A, Schaeffer L and Zhou J 2016 An investigation on the properties of injection-molded pure iron potentially for biodegradable stent application *Powder Technology* **294** 226-35
[9] Li Y, Liu S, Qu X and Huang B 2003 Thermal debinding processing of 316L stainless steel powder injection molding compacts *Journal of Materials Processing Technology* **137** 65-9
[10] Omar M A, Ibrahim R, Sidik M I, Mustapha M and Mohamad M 2003 Rapid debinding of 316L stainless steel injection moulded component *Journal of Materials Processing Technology* **140** 397-400
[11] Enneti R K, Shivashankar T S, Park S-J, German R M and Atre S V 2012 Master debinding curves for solvent extraction of binders in powder injection molding *Powder Technology* **228** 14-7
[12] Setasuwon P, Bunchavimonchet A and Danchaivijit S 2008 The effects of binder components in wax/oil systems for metal injection molding *Journal of Materials Processing Technology* **196** 94-100
[13] Gorjan L, Kosmač T and Dakskobler A 2014 Single-step wick-debinding and sintering for powder injection molding *Ceramics International* **40** 887-91
[14] Hayat M D, Wen G, Zulkifli M F and Cao P 2015 Effect of PEG molecular weight on rheological properties of Ti-MIM feedstocks and water debinding behaviour *Powder Technology* **270** 296-301
[15] Shbeh M M and Goodall R 2015 Design of water debinding and dissolution stages of metal injection moulded porous Ti foam production *Materials & Design* **87** 295-302
[16] Aslam M, Ahmad F, Yusoff P S M B M, Altaf K, Omar M A and M.German R 2016 Powder injection molding of biocompatible stainless steel biodevices *Powder Technology* **295** 84-95
[17] Zaky M T, Soliman F S and Farag A S 2009 Influence of paraffin wax characteristics on the formulation of wax-based binders and their debinding from green molded parts using two comparative techniques *Journal of Materials Processing Technology* **209** 5981-9
[18] Md Ani S, Muchtar A, Muhamad N and Ghani J A 2014 Binder removal via a two-stage debinding process for ceramic injection molding parts *Ceramics International* **40** 2819-24
[19] Gorjan L, Dakskobler A and kosmač T 2010 Partial wick-debinding of low-pressure powder injection-moulded ceramic parts *Journal of the European Ceramic Society* **30** 3013-21
[20] Cheng J, Wan L, Cai Y, Zhu J, Song P and Dong J 2010 Fabrication of W–20 wt.%Cu alloys by powder injection molding *Journal of Materials Processing Technology* **210** 137-42
[21] Raza M R, Ahmad F, Omar M A and German R M 2012 Effects of cooling rate on mechanical properties and corrosion resistance of vacuum sintered powder injection molded 316L stainless steel *Journal of Materials Processing Technology* **212** 164-70
[22] Farhan M F, Hamidi A, Sharuzi W, Harun W, Faiz A and Abu Bakar S 2016 Effect of Binders on Physical and Mechanical Properties of Stainless Steel 316L Alloy Fabricated by Metal Injection Moulding Process